Available online at www.sciencedirect.com
SCIENCE DIRECT®
Journal of Nuclear Materials 346 (2005) 98–108
journal of nuclear materials
www.elsevier.com/locate/jnucmat

Hydride fuel behavior in LWRs

Donald R. Olander *, Marowen Ng

Department of Nuclear Engineering, University of California, Berkeley, CA 94720-1730, USA

Received 12 July 2004; accepted 11 May 2005

Abstract

The U–Zr hydride $U_{0.31}ZrH_{1.6}$ offers a number of advantages over oxide fuel for light-water reactors. Fission-gas release appears to be very small (release fraction $\sim 10^{-4}$) up to 600 °C, which is close to the maximum fuel temperature. Initial irradiation-induced swelling can be as large as 5% for temperatures exceeding 650 °C. Hydrogen redistributes due to the non-uniform temperature in the fuel from the as-fabricated H/Zr of 1.6 to one that is higher at the pellet periphery than at the centerline. Radial redistribution produces 'hydrogen' stresses in the pellet which add to the usual thermal stresses. In a helium-bonded fuel rod, the total stresses are less than the fracture stress; in a liquid-metal-bonded fuel rod, the fracture stress is exceeded in the central portion of the pellet, but the surface remains in compression. Axial redistribution moves substantial quantities of hydrogen from the middle portion of the fuel stack to the ends. The neutronic effect of this displacement of the moderator is unknown.

1. Introduction

Use of uranium–zirconium hydride as the fuel for light-water reactors offers a number of advantages over uranium dioxide or uranium–plutonium dioxide [1]. Chief among these are the reduced volume of water needed in the hydride-fueled core because moderation occurs in the fuel pellet proper, and the more rapid neutronic response to transients, also the result of commingling of fuel and moderator. The former feature permits a significant reduction in the size of the coolant channels, thereby reducing the core size for a given power. The latter property has long been exploited in pulsing TRIGA reactors [2]. As a fuel in light-water reactors (LWRs), it provides a safety feature absent in oxide fuel.

In the proposed hydride fuel, uranium is present as metallic inclusions in a matrix of $ZrH_{1.6}$.[1] Fig. 1 is a micrograph of unirradiated fuel with 45 wt% U (on a total metal basis), or a volume fraction of 0.21. The microstructure consists of uranium particles of indeterminate shape but with characteristic dimensions of ~ 5 μm dispersed in zirconium hydride of unknown structure. The uranium content is 45 wt%,. The enrichment is 20% ^{235}U in order to minimize the fraction of uranium in the fuel. The chemical formula is $U_{0.31}ZrH_{1.6}$, which corresponds to a Zr/U atom ratio of 3.2 and an H/Zr atom ratio of 1.6. This hydrogen content is chosen for several reasons: (i) it provides sufficient hydrogen for the purposes described in the preceding paragraph; (ii) at operating temperatures (as a

* Corresponding author. Tel.: +1 510 642 7055; fax: +1 510 643 9685.
E-mail address: fuelpr@socrates.berkeley.edu (D.R. Olander).

[1] Because of the low dissociation temperature of UH_3 at the hydrogen pressures employed during fuel fabrication, the stable form of uranium is the metal.

0022-3115/$ - see front matter © 2005 Elsevier B.V. All rights reserved.
doi:10.1016/j.jnucmat.2005.05.017

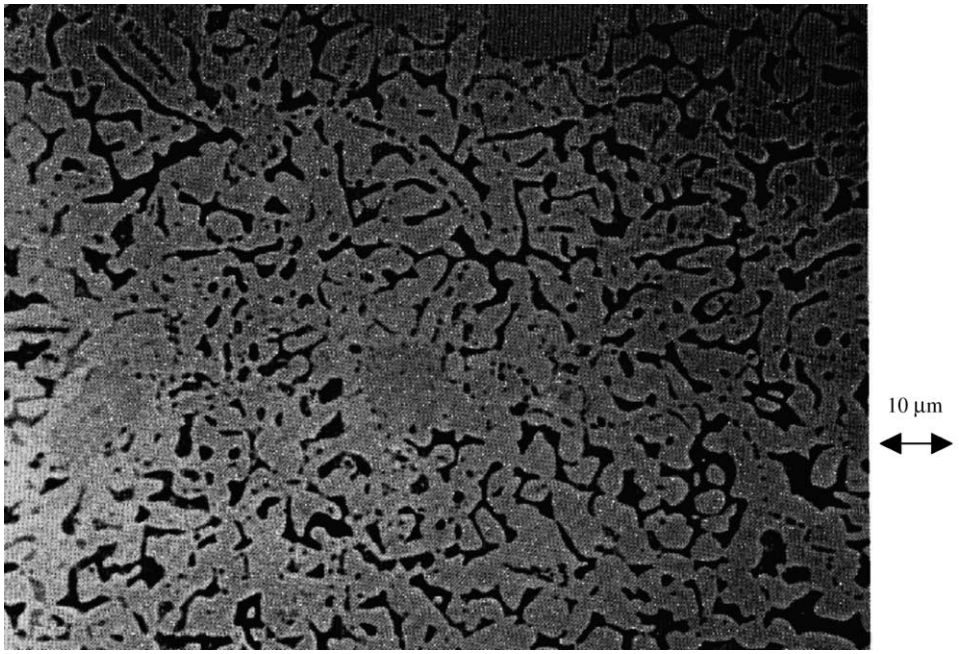

Fig. 1. Microstructure of unirradiated $U_{0.31}ZrH_{1.6}$ (from [3]). Black areas are uranium metal; $ZrH_{1.6}$ is gray.

power-reactor fuel) the hydrogen gas overpressure is manageable; (iii) it places the system squarely in the δ-hydride region of the Zr–H phase diagram.

Table 1 shows the thermal characteristics of the hydride fuel in three configurations. The first two apply to the hydride fuel as a replacement for oxide fuel in LWRs. The thermal characteristics are intended to represent conditions at the midplane of a rod located in an assembly close to the center of the core.

The last column provides similar information for the 'power TRIGA' currently operating in Romania [4]. This version differs from all other TRIGA research reactors in its steady-state power of 14 MW and in its use of forced-convection cooling. Most of the standard TRIGAs operate at 1 MW and are cooled by natural convection of pool water. The fuel of the Romanian TRIGA was reported to have been irradiated to a burnup of 60 MW d/kg U [4].

The two versions of the hydride fuel element for LWR usage shown in Table 1 differ only in the material that fills the fuel-cladding gap. The advantages of using the low-melting liquid metal (LM) stem from the elimination of the thermal resistance of the fuel-cladding gap. The benefits of the LM bond in oxide fuel elements are

Table 1
Operating characteristics at the midplane of a hydride fuel element in a maximum power assembly

Characteristic	LWR – helium	LWR – liquid metal	Romanian TRIGA
Fuel-cladding gap bond			
Fuel composition	$U_{0.31}ZrH_{1.6}$	$U_{0.31}ZrH_{1.6}$	$U_{0.31}ZrH_{1.6}$
Fuel pellet OD, mm	12	12	12
Peak LHR, W/cm	375	375	800
Fuel centerline, °C	680	555	820
ΔT_{fuel}, °C	170	170	360
ΔT_{gap}, °C	125[a]	1[a]	250
$\Delta T_{cladding}$, °C	46[b]	46[b]	60[c]
ΔT_{fluid}, °C	39	39	90
$T_{coolant}$, °C	300	300	60

[a] For a gap thickness of 35 μm.
[b] Zircaloy.
[c] Inconel.

given in Ref. [5]. For hydride fuel elements, the LM is essential in order to accommodate the large irradiation-induced swelling of the fuel (see below).

2. Irradiation behavior

Data on the irradiation behavior of hydride fuels in conditions representative of LWRs are scarce. Fission-gas release measurements were made as part of NASA's space reactor program (1960–1970) [6]; later irradiation tests were performed by General Atomics, the supplier of TRIGA research reactor fuel (1966–1977) [2]; long-term irradiation in the Oak Ridge Research Reactor (ORR) and post-irradiation examination were conducted at the Oak Ridge National laboratory [7].

Many of the experiments are of unknown quality and are poorly documented. Neither the Zr/U ratio nor the H/Zr ratio is known for many of the tests. Both in-pile measurements of the release-to-birth rate ratio of ^{85}Kr and post-irradiation anneal experiments on several radioactive fission gases are contained in Fig. 2. However, the in-pile experiments only sample release from a ~10 μm-thick layer at surface.

In the post-irradiation anneal experiments, the anneal temperature is given but the irradiation temperature and the annealing time are not. The 'fraction release' is not defined. Because of the two-phase microstructure of the fuel, the Booth model is not applicable; some of the fission fragments from the U phase are stopped in the ZrH_x matrix. Gas bubbles were not reported and no modeling was attempted.

Despite the shortcomings of the experiments cited above, all agree that gas release up to ~600 °C is solely by recoil. Even at fuel temperatures of 800 °C in the Power TRIGA [4], the fission-gas release fraction is much lower than that for oxide fuels at their maximum temperature of ~1500 °C.

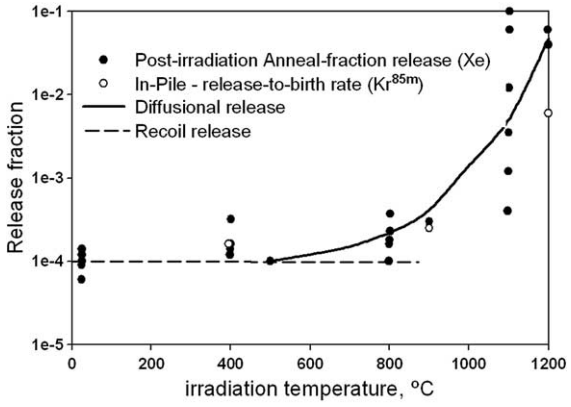

Fig. 2. Summary of numerous fission gas release measurements during or following reactor irradiation (in the postirradiation anneal tests, the abscissa is the anneal temperature); the horizontal dashed line is the calculated recoil release fraction for the 12 mm diameter fuel pellet (from Refs. [2,7,9]).

The results of the 920-day irradiation of 3.8 cm – diameter TRIGA fuel in the ORR supports the earlier findings of low fission-gas release [7]. In these tests, $U_{0.31}ZrH_{1.6}$ with a ^{235}U enrichment of 20% was irradiated at a rod-average linear heat rating (LHR) of 980 W/cm to a burnup of 65% of the initial ^{235}U (or 125 MW d/kg U.[2]) There was no detectable pressure rise inside the fuel rod. The reported fission-gas release fraction of 4×10^{-4} was based on the calculated maximum fuel temperature of 650 °C and a conservative reading of Fig. 2.

Very recent fission-gas release measurements on hydride fuel were conducted at the Argonne National Laboratory as part of the Department of Energy's program of conversion of TRIGA fuel from high enrichment uranium to fuel with 20% ^{235}U [8]. This last set of results is not included in Fig. 2 because the release tests were conducted in a short-time temperature ramp.

The swelling behavior of hydride fuel is shown in Fig. 3. Neither Refs. [2] nor [9] cite the source of these plots other than implying that they were obtained from NASA's Space Nuclear Auxiliary Power (SNAP) program [6] and from measurements on spent TRIGA fuel. As with the fission-gas release information, the details of the experiments that lie behind the swelling plots are not available. Of particular interest is the method used to separate LHR and temperature in irradiation tests. Unless sophisticated methods are applied to separate them, these two parameters track each other.

The most striking feature of the swelling plots is the rapid increase at burnups less than 4 MW d/kg U.[3] Ref. [9] attributes the rapid initial swelling to voids in the ZrH_x matrix. The voids are supposedly created by condensation of irradiation-produced vacancies, which is the mechanism that creates voids in stainless steel in fast breeder reactors or fusion reactors. However, this explanation is not supported by irradiation tests of non-fuel $ZrH_{1.85}$ by Shcherbak et al. [10]. In this work, pure hydrides were irradiated at temperatures from 430 to 530 °C. At a fluence of 0.6×10^{26} n/m^2 ($E_n > 0.1$ MeV), swelling due to void formation was 0.7%; at 3×10^{26} n/m^2, it was 5%. However, these fluences far

[2] see Appendix B for explanation of the different burnup units applied to hydride fuels.

[3] The common burnup unit used in the older reports is '% on a total metal atom basis'. Conversion to the modern energy-based burnup units depends on the zirconium-to-uranium ratio of the fuel (see Appendix B). Unfortunately, the references in which the plots of Fig. 3 appear do not give U/Zr ratio, or, equivalently, the wt% U. For 10 wt% U the end of the rapid growth occurs at 23 MW d/kg U; for 45 wt% U it is 4 MW d/kg U. The latter figure has been used in unit conversion.

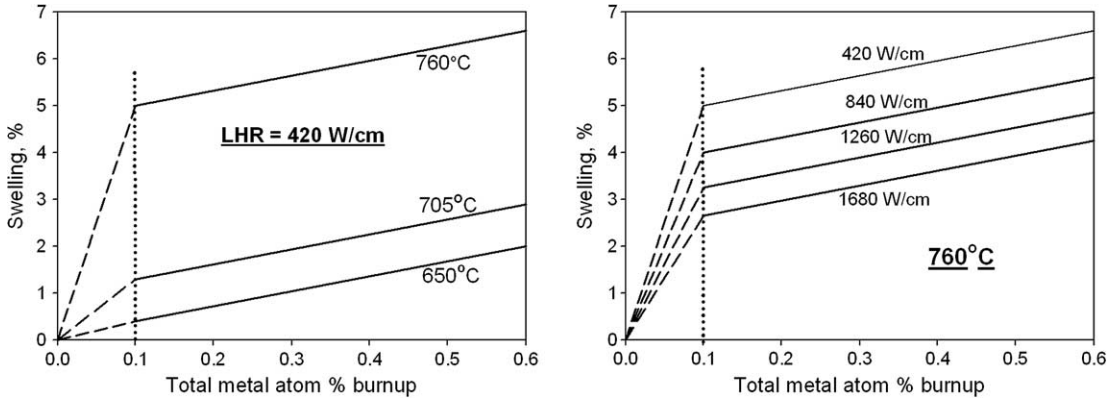

Fig. 3. Swelling of hydride fuel as a function of burnup, temperature and LHR (from Refs. [2,9]).

exceed the thermal-neutron fluence corresponding to the 4 MW d/kg U burnup below which the anomalous swelling is seen in Fig. 3; the 920-day irradiation of fuel with 45 wt% U to a burnup of 4 MW d/kg U is equivalent to a fractional consumption of the ^{235}U of 0.021 (from Appendix B). This quantity is also equal to $1-\exp(-\sigma_{25}^{\text{fiss}}\varphi t)$, where $\sigma_{25}^{\text{fiss}} \sim 500$ barns is the fission cross-section of ^{235}U and φt is the thermal-neutron fluence. Thus the end of the rapid swelling period occurs at a thermal-neutron fluence of 4×10^{23} n/m^2. If the fast fluence in the ORR is of this magnitude, the fluence that creates 0.7 vol.% voids in pure hydride [10] is two orders of magnitude greater than that in the hydride fuel used in the irradiations at Oak Ridge [7]. The mechanism of the anomalous early swelling in hydride fuel, if it is indeed real, remains unknown.

Whatever the cause, the abnormal swelling behavior appears only at temperatures above 650 °C. This may be a significant design restraint: either the temperature is kept well below the critical value or a large initial fuel-cladding gap is needed.

3. Temperature distribution the in the fuel

Available experimental evidence shows no temperature dependence of the thermal conductivity of ZrH_x, which is 5–6 times larger than that of UO_2 [11]. The room-temperature thermal conductivity varies slightly with the H/Zr ratio, decreasing from 0.18 W/cm K in $ZrH_{1.5}$ to 0.16 W/cm K in $ZrH_{1.7}$ [11]. However, the scatter of these data is large enough to warrant the conclusion that the thermal conductivity is independent of H/Zr. In addition, a single-line comment in Ref. [2] claims that the thermal conductivity is also independent of uranium content.

For constant thermal conductivity, the temperature distribution as a function of radius r is determined by the expression:

$$\frac{T(r)-T_s}{T_0-T_s}=1-\left(\frac{r}{R}\right)^2, \tag{1}$$

r = radial position in the pellet; R = fuel radius; T_s = fuel surface temperature; T_0 = fuel centerline temperature.

The simple parabolic temperature distribution neglects the effect of burnup on the thermal conductivity. For the present analysis, the fuel centerline and surface temperatures are given in Table 1.

4. Hydrogen redistribution

The properties of the hydride fuel should depend on the presence of 21 vol.% uranium in the ZrH_x matrix. Some undoubtedly do, but other properties, such as the thermal conductivity, appear to be unaffected by the presence of metallic uranium. Since the uranium phase contains no hydrogen,[1] all redistribution analyses, including the present one, consider the fuel as pure $ZrH_{1.6}$ [12,13].

Redistribution of hydrogen in metal hydrides is analogous to oxygen redistribution in the mixed-oxide fuel of fast-breeder reactors. In both cases, the moving species (H or O^{2-}) migrates to the cold periphery of the fuel pellet. In the case of H in ZrH_x, the ΔT from the centerline to the periphery of the fuel (~170 °C) is low compared to that in oxide fuel (~800 °C); however, the property responsible for redistribution in a temperature gradient is thermal diffusion. This property, in the form of the heat of transport is substantial for H in ZrH_x and the large ordinary diffusion coefficient of H in the hydride insures that the steady-state distribution is attained quickly.

As long as hydrogen remains in the fuel, there are no neutronic consequences of redistributing hydrogen radially (axial redistribution is a different story; see later). However, increasing the H/Zr ratio at surfaces exposed

to the free volume in the fuel element increases the rate of hydrogen loss from the fuel. The stress state in the pellet is affected by the temperature gradient and the resulting radial redistribution of hydrogen. This issue is addressed in subsequent sections.

Redistribution of hydrogen in cylindrical pellets of ZrH_x is calculated for the parabolic temperature distribution of Eq. (1) with the bounding temperatures given in Table 1. The constraints on the calculation are: (i) the average H/Zr ratio of the solid does not change; (ii) the fuel-cladding gap is filled either with helium or a low-melting liquid metal; (iii) the system has achieved a steady state, so the gradient of the flux is zero, or the flux is constant. The radial flux of hydrogen in the hydride is given by

$$J_r = -D_S\left(\frac{dC_S}{dr} + \frac{T_Q}{T}\frac{C_S}{T}\frac{dT}{dr}\right) = -D_S\frac{\rho_{Zr}}{M_{Zr}}\left(\frac{dC}{dr} + \frac{T_Q}{T}\frac{C}{T}\frac{dT}{dr}\right), \quad (2)$$

D_S = diffusion coefficient of hydrogen in the hydride, cm^2/s; C_S = concentration of hydrogen in the solid, mol H/cm^3; T_Q = heat of transport of H in the hydride divided by the gas constant, K; T = temperature, K; ρ_{Zr} = density of zirconium in $ZrH_{1.6}$, g/cm^3; M_{Zr} = atomic weight of Zr; C = H/Zr atomic ratio.

The terms in parentheses represent ordinary and thermal diffusion, respectively. The second equality in Eq. (2) comes from conversion of the volumetric concentration of hydrogen, C_S, to the H/Zr ratio, C.

Since loss of hydrogen from the pellet is neglected, $J_r = 0$, and the solution to Eq. (2) is

$$C = Ae^{T_Q/T} = Ae^{B\theta}, \quad (3)$$

where $B = T_Q/T_0$ is the dimensionless heat of transport and $\theta = T_0/T$ is a dimensionless inverse temperature. The constant of integration A is determined from the specified average H/Zr ratio of the fuel:

$$C_{avg} = \frac{2}{R^2}\int_0^R rC(r)dr. \quad (4)$$

In dimensionless terms, Eq. (1) is

$$\frac{\theta^{-1} - \theta_S^{-1}}{1 - \theta_S^{-1}} = 1 - \left(\frac{r}{R}\right)^2, \quad (5)$$

where $\theta_S = T_0/T_S$, the ratio of the centerline and surface temperatures. The integral in Eq. (4) can be converted from r to θ using Eq. (5), resulting in:

$$C_{avg} = \frac{\theta_S}{\theta_S - 1}\int_1^{\theta_S}\frac{C(\theta)}{\theta^2}d\theta = \frac{\theta_S}{\theta_S - 1}A\int_1^{\theta_S}\frac{e^{B\theta}}{\theta^2}d\theta. \quad (6)$$

The analysis is performed for fuel elements with helium and with liquid metal in the fuel-cladding gap. The fuel centerline and surface temperatures for these two gap fillers are given in Table 1. The heat of transport of H in ZrH_x is 640 K [14].

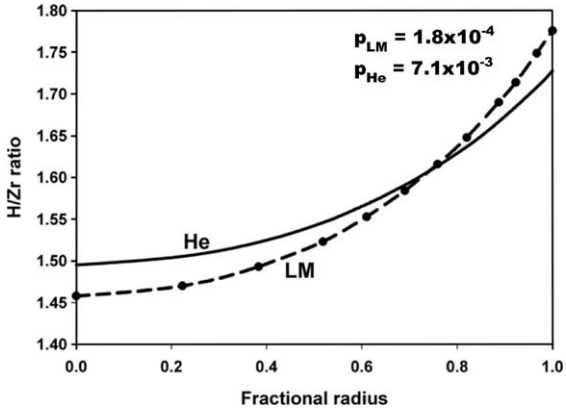

Fig. 4. Hydrogen redistribution in the fuel pellet operated under conditions given in Table 1. For gas and liquid metal gap fillers. The equilibrium hydrogen pressures at the fuel surface are shown.

Fig. 4 illustrates the most significant feature of the redistribution phenomenon, namely accumulation of hydrogen at the fuel surface and depletion at the center. Despite the lower temperatures, the LM bond causes greater hydrogen redistribution than the He bond. Using Eq. (1) for the temperature and Fig. 4 for the H/Zr ratio C, the hydrogen partial pressure, p (in atm), is obtained from [15,16]:

$$\ln p = 2\ln\left(\frac{C}{2-C}\right) + 8.01 + 5.21C - \frac{2.0\times10^4}{T}. \quad (7)$$

For each gap-fill material, Fig. 4 shows the equilibrium hydrogen partial pressures at the periphery of the fuel. The hydrogen partial pressures are small compared to typical fuel-element filling gas pressures, so during normal operation, hydrogen does not contribute to internal pressurization of the fuel rod.

However the H_2 partial pressure could be high enough to significantly reduce the H/Zr ratio of the fuel by loss to the free volume in the rod, which includes the gap and the plenum. These two volumes are at different temperatures; the average temperature of the gas in the gap is ~400 °C and in the plenum, it is ~320 °C. The volume of the plenum is ~20 cm^3 and the volume of an 80 μm thick gap associated with the entire length of a 425 cm-length fuel stack is also ~20 cm^3. For the purposes of this calculation, combine the two gas volumes by first raising the temperature of the plenum from 320 °C to 400 °C, so that the volume of the plenum gas is now ~23 cm^3. The result is a gas volume of ~43 cm^3 at a temperature of 400 °C. The equilibrium hydrogen pressure at the fuel surface is taken from Fig. 4 (7×10^{-3} atm). From the ideal gas law, the gas contains $\sim5\times10^{-6}$ mol of H_2, or $\sim10^{-5}$ mol of H. The volume of solid hydride fuel is ~335 cm^3, of which 79% is $ZrH_{1.6}$ (metallic uranium occupies the remaining 21%). The

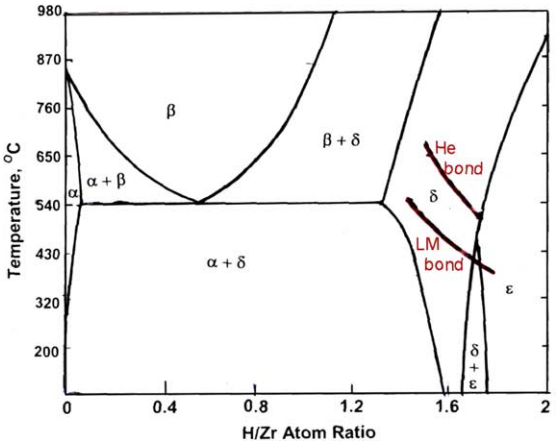

Fig. 5. Hydrogen redistribution trajectories superimposed on the Zr–H phase diagram.

density of Zr in the hydride is ~0.06 mol Zr/cm^3, so the fuel stack contains ~16 mol of Zr. The quantity of H associated with this quantity of Zr is 25 mol, compared to which the 10^{-5} mol in the gas phase is negligible. The H/Zr ratio of the fuel is unaffected by the maximum conceivable loss of hydrogen to the gas phase in the fuel rod.

The traces of the redistributed hydrogen are shown on the H–Zr phase diagram in Fig. 5. The He-bonded case falls totally in the δ region of the phase diagram. The low temperature zone of the LM-bonded case is in the ε phase. The properties of this phase of the H–Zr system (e.g., thermal conductivity, heat of transport, irradiation effects) are unknown. Huang et al. [13] claim that fission product swelling is greater in the δ + ε two-phase region, with the concomitant possibility of fuel cracking.

A second hydrogen loss mechanism is absorption in or permeation through the cladding. Simple analysis shows that absorption in unprotected Zircaloy cladding is excessive. Three remedies are feasible: providing a hydrogen-impervious coating on the cladding inside wall; converting of a few tens of microns of the pellet surface to ZrO_2 during fabrication [17]; or using a liquid metal in the fuel-cladding gap.

5. Thermal stresses

Thermal stresses in the pellet are calculated using the parabolic temperature distribution of Eq. (1). The usual textbook equations for these stresses cannot be used because the thermal expansion coefficient is a function of temperature:

$$\alpha = \alpha_0[1 + aT], \tag{8}$$

where a is a constant and T is the temperature in celsius. The stress analysis, modified to account for this variation, is given in Appendix A. Properties of ZrH_x are:

- Thermal expansion coefficient (Ref. [2]): $\alpha_0 = 7.4 \times 10^{-6}\ ^\circ C^{-1}$, $a = 2 \times 10^{-3}\ ^\circ C^{-1}$.
- Young's modulus $E = 130$ GPa; Poisson's ratio $v = 0.32$ (Ref. [2]). $E\alpha_0\Delta T_0/(1 - v) = 221$ MPa.
- Fracture stress: 200 MPa for ZrH_1 (Ref. [18]).

The fracture stress from Ref. [18] is the result of a partially-successful test at room temperature. The effects on the fracture stress of increasing the H/Zr ratio from 1 to 1.6 and increasing the temperature from 25 °C to 600 °C are unknown.

Fig. 6 compares the axial and hoop stress profiles in the pellet for the helium-bonded rod for the

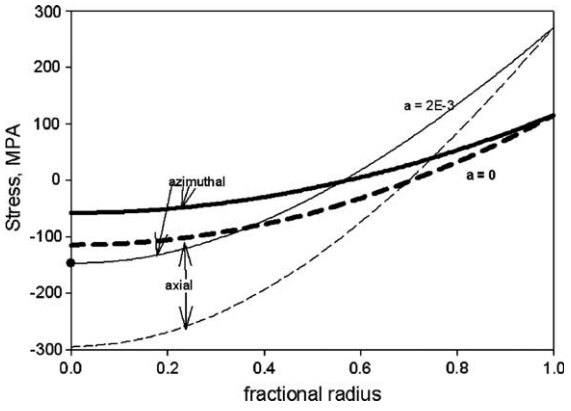

Fig. 6. Thermal stress distribution in a hydride fuel pellet with a helium-bonded gap. Light curves: with temperature-dependent α; heavy curves: constant α.

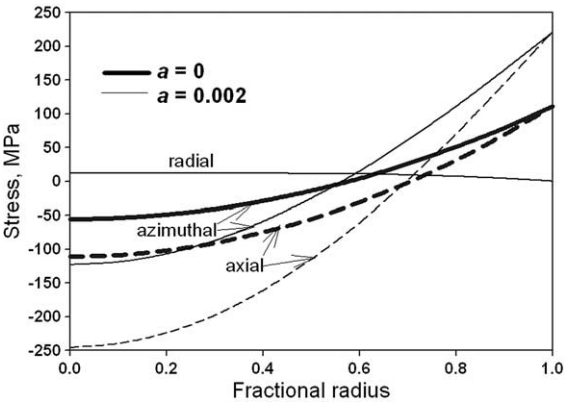

Fig. 7. Thermal stresses in a hydride fuel pellet with liquid metal in the gap. Light curves: with temperature-dependent α; heavy curves: constant α.

conventional constant – α case and for the present case wherein the parameter a is not zero. The latter significantly enhances the stress variations with r/R.

With a liquid metal in the gap, the only change is uniform reduction of the fuel temperature by 125 °C. Fig. 7 shows the thermal stress distribution for this case. The stresses are slightly lower than the He-bonded case in Fig. 6, but the effect of the temperature-dependent α is the same.

6. Hydrogen stresses

In addition to the thermal stresses induced by the variable temperature, another source of stress arises from the change of density of the hydride with the hydrogen content. This feature, when combined with H redistribution, generates 'hydrogen stresses'.

The density of (U,Zr)H_C decreases, and the material expands, as the H/Zr ratio increases. For hydrides with $C < 1.3$ at room temperature, Merten et al. [18] found the density to follow: 6.83–0.55C g/cm^3. This expression can be converted to a molar density by dividing by $91 + C$. Inverting this quotient gives the molar volume as $13.3(1 + 0.092\ C)$ cm^3/mol. This formula can be converted to the fractional volume change $(V - V_{\text{ref}})/V_{\text{ref}}$ where V_{ref} is the molar volume for $C = 1.6$. Taking 1/3 of the fractional volume change gives the *linear coefficient of hydrogen expansion* β:

$$\frac{\Delta L}{L} = \frac{1}{3} \times \frac{13.3 \times 0.092(C - 1.6)}{13.3(1 + 0.092 \times 1.6)} = \beta(C - 1.6), \tag{9}$$

where $\beta = 0.027$. Gylfe et al. [19] give approximately the same value of β for $1.64 \leqslant C \leqslant 1.94$. Simnad [2] reports density variation with C that changes slope at the δ/ε phase boundary. In the δ phase, the value of β is about the same as the value cited above.

The hydrogen-induced stress analysis is identical to the conventional thermal-stress analysis for constant α [20]. The only change is replacement of $\alpha\Delta T$ with $\beta\Delta C$, T by C and r/R with $y^{1/2}$. The azimuthal stress is

$$\frac{\sigma_\theta^{\text{H}}}{\left(\frac{\beta E}{1-\nu}\right)} = S_\theta^{\text{H}} = \frac{1}{2}\int_0^1 C(y)\mathrm{d}y + \frac{1}{2y}\int_0^y C(y')\mathrm{d}y' - C(y). \tag{10}$$

In order to evaluate the integrals in Eq. (10), the curves in Fig. 4 are fitted to parabolas; for the He-bonded rod, the H/Zr profile is approximated by

$$C(y) = 1.515 + 0.151y + 0.044y^2. \tag{11}$$

Substituting Eq. (11) into Eq. (10) yields the dimensionless azimuthal stress:

$$S_\theta^{\text{H}} = 0.045 - 0.113y - 0.037y^2. \tag{12}$$

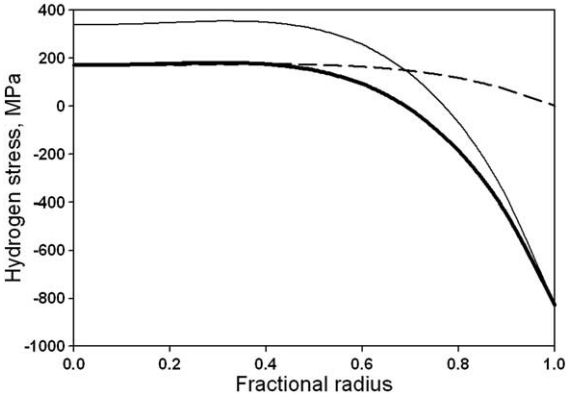

Fig. 8. Hydrogen stresses in a fuel pellet with a helium-bonded gap.

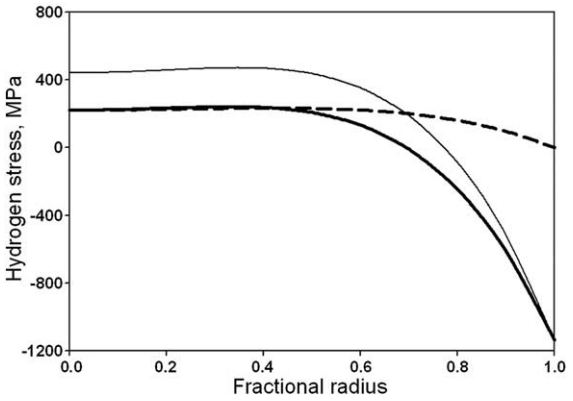

Fig. 9. Hydrogen stresses in a fuel pellet with a LM-bonded gap.

Proceeding in a similar fashion, the remaining two hydrogen stress components are

$$S_r^{\text{H}} = 0.045 - 0.038y - 0.0073y^2;$$
$$S_z^{\text{H}} = 0.090 - 0.151y - 0.044y^2. \tag{13}$$

The same procedure is applied for liquid metal in the gap. The hydrogen stress distributions are plotted in Figs. 8 and 9 for these two cases. As expected, the stress components are compressive at the periphery and tensile at the center. The magnitudes of the stress components are larger in the LM-bonded rods.

7. Total stresses

If the sum of the thermal and hydrogen stresses exceeds the fracture stress (in tension) at the pellet periphery, cracking occurs. The total stress is

$$\sigma_i^{\text{tot}} = \sigma_i^{\text{th}} + \sigma_i^{\text{H}}, \tag{14}$$

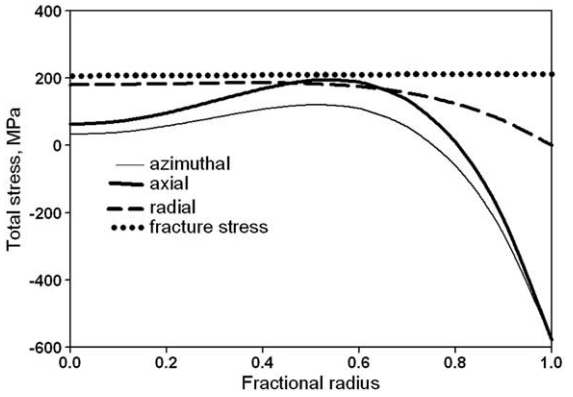

Fig. 10. Sum of thermal and hydrogen stresses in a He-bonded fuel rod.

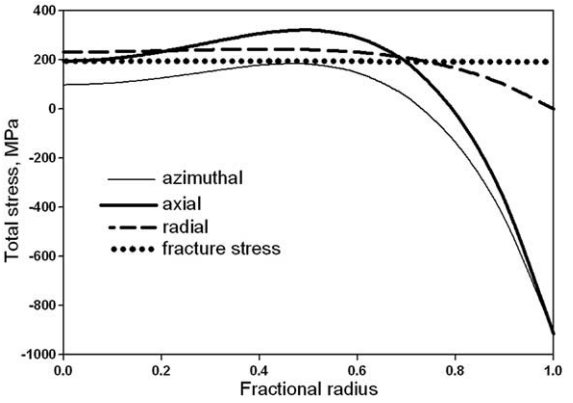

Fig. 11. Sum of thermal and hydrogen stresses in a LM-bonded fuel rod.

where i is r, θ, or z. The radial distributions of the total stresses are shown in Figs. 10 and 11. In the LM-bonded case, the nominal fracture stress is exceeded by the axial component of the combined stress over a fractional radius interval from 0.2 to 0.7.

The maximum tensile stress is 322 MPa at $r/R = 0.5$. Although the nominal fracture stress is exceeded in the interior of the pellet, it is unlikely that cracking will occur because this region is surrounded by zones of compressive stress. The azimuthal and axial components are larger than the fracture stress at the pellet periphery; however, damage is unlikely because these components are compressive.

8. Axial redistribution

Of greater consequence than radial hydrogen distribution in fuel pellets to the neutronic performance of a hydride-fueled reactor is movement of hydrogen axially. The former occurs on the scale of millimeters, and its neutronic effect, if any, is effectively that of a small-scale heterogeneity. Axial hydrogen redistribution, on the other hand, displaces large quantities of hydrogen over distances of meters. Loss of moderating power in the hydrogen-impoverished zone near the fuel-element midplane may or may not be adequately compensated by the higher hydrogen content of the fuel at the top and bottom of the fuel stack.

With the r, z temperature distribution in the fuel specified, axial hydrogen redistribution is inseparable from radial redistribution. Determination of $C(r, z)$ requires solution the diffusion equation (including thermal diffusion) in two spatial dimensions and time. Although steady state is quickly achieved in the radial direction [13], it is not a priori obvious that the axial steady state is attainable within, say, a reactor cycle. In addition, the discontinuous nature of the fuel stack could result in a rate-limiting kinetic step associated with transfer of hydrogen via the gas phase in the pellet–pellet interfaces. This is not likely because the overall process is so slow that gas–solid equilibration at the pellet faces is probably attained. However, the worst case (neutronically) is the steady state, so this condition is assumed in the following analysis. Solution of the two-spatial dimension diffusion problem is complicated by the vast difference in the characteristic lengths in the two directions. This effect appears in the non-dimensionalized diffusion equation as the square of the ratio of the pellet radius to the half-height of the fuel stack. This ratio is on the order of 10^{-5} and multiplies the axial diffusion term in the conservation equation.

A simpler, approximate method is as follows:

1. The thermal state is specified by selection of the inlet coolant temperature and the relative axial variation of the linear heat rating, LHR(z)/LHR(0), $-L \leqslant z \leqslant L$, where $2L$ is the height of the fuel stack. A typical PWR axial power shape is shown in Fig. 12.

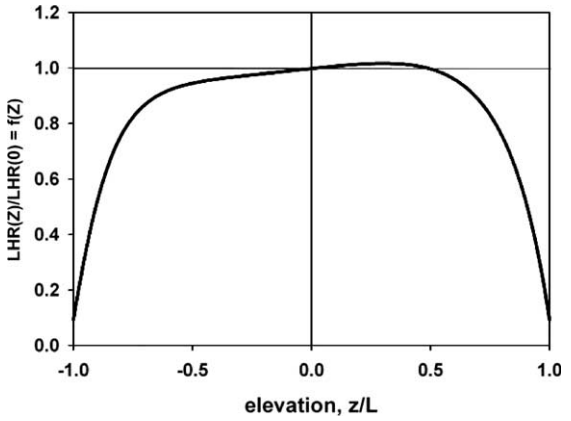

Fig. 12. Typical axial power distribution in a PWR. The height of the fuel stack is 3.7 m (Ref. [21]).

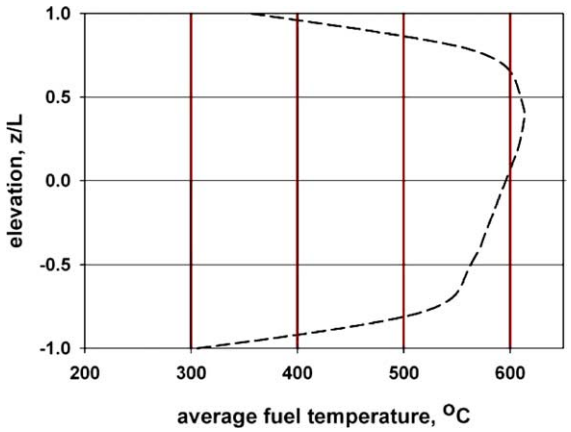

Fig. 13. Axial variation of the radially-averaged fuel temperature.

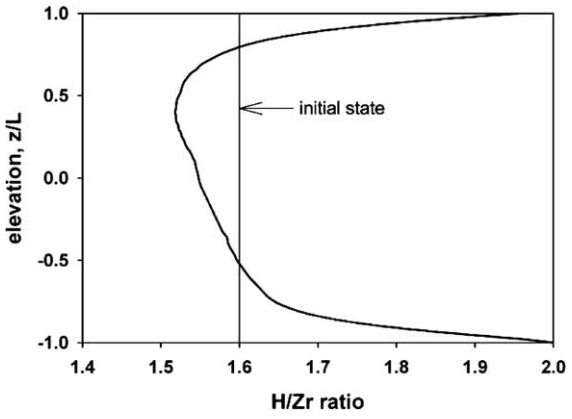

Fig. 14. Axial H/Zr profile at steady state.

For a coolant temperature of 300 °C at the midplane (the value in Table 1), the inlet temperature is 275 °C and the temperature rise through the core is 50 °C. The fuel surface and centerline temperatures are fixed by hooking the axial solution to the conditions given in Table 1 (for the He-bonded case) at $z = 0$.

2. Axial hydrogen redistribution is assumed to be driven by the radially-averaged fuel temperature as a function of z (Fig. 13).
3. In order to prevent the calculated H/Zr ratio from exceeding 2.0, the heat of transport (in Kelvins) is forced to approach zero as H/Zr $\rightarrow$ 2 according to the function

$$1.34(2-\overline{C})^{0.32}.$$

This function has two features: first, it is unity at $\overline{C} = 1.6$; second, it approaches zero as $\overline{C} \rightarrow 2$. The first characteristic recovers the literature value of the heat of transport ($T_Q = 640$ K). The second prevents H/Zr rations greater than 2 from being calculated. With this modification, the condition of zero hydrogen flux along the length of the fuel stack (because no hydrogen escapes from the ends) is the z analog of the expression in parentheses in Eq. (2):

$$\frac{\mathrm{d}\overline{C}}{\mathrm{d}z} = -1.34T_Q(2-\overline{C})^{0.32}\overline{C}\frac{\mathrm{d}\overline{T}}{\overline{T}^2}. \tag{15}$$

Eq. (16) is solved numerically using an initial condition $\overline{C}(-L)$ that produces the correct overall average H/Zr ratio:

$$\frac{1}{2L}\int_{-L}^{L}\overline{C}(z)\mathrm{d}z = 1.6. \tag{16}$$

The resulting hydrogen redistribution profile, with $\overline{C}(-L) = 1.9999$, is shown in Fig. 14. All of the hydrogen in the region beneath the H/Zr = 1.6 line has been moved to the top and bottom of the fuel stack.

Whether the final hydrogen distribution of Fig. 14 can be achieved in a typical in-reactor fuel lifetime of 6 years can be roughly estimated as follows. In transient diffusion problems, steady state is ~75% attained when $Dt/L^2 \sim 2$. Taking $D \approx 3\times10^{-5}$ cm^2/s and $L = 185$ cm gives a time of 75 years. However, for the following reasons, this estimate should not be accepted until a full transient analysis of the problem is performed: (i) the above estimation method is not valid when thermal diffusion accompanies ordinary diffusion; (ii) the strong radial and axial temperature variations make the estimate of D very uncertain; (iii) only one set of thermal conditions has been analyzed; although typical of current LWRs, other conditions may be more conducive to hydrogen movement.

9. Conclusions

Several in-reactor behavior features of the $U_{0.31}ZrH_{1.6}$ power-reactor fuel have been analyzed and their effects on fuel performance assessed.

Fission-gas release appears to be very small, even for irradiations to high burnups. Fission product swelling, on the other hand, shows a very large initial increase at temperatures exceeding 650 °C. This last feature, rather than hydrogen loss, may fix the maximum fuel temperature.

A process that has no analog in oxide LWR fuel is hydrogen redistribution driven by solid-state thermal diffusion. This process results in increase of the H/Zr ratio at the pellet periphery with concomitant impoverishment at the fuel centerline.

Under normal operating conditions with He in the gap, loss of H from the fuel by transfer to the gas in the plenum and the gap is negligible. On the other hand, a transient that pushes fuel temperatures above 1000 °C could release significant quantities of hydrogen. The

kinetics of this desorption process have not been studied, nor has the rate of the subsequent re-absorption step following cool-down.

Transients in fuel rods with an LM-bonded gap are altogether different. Hydrogen loss from accidents short of cladding burst is impossible. The equilibrium hydrogen pressure would have to exceed the internal rod total pressure in order to force H_2 gas through the liquid metal and into the plenum. The temperatures required to generate the necessary tens of atm of H_2 are well over 1500 °C.

Accumulation of hydrogen at the fuel surface will damage unprotected Zircaloy cladding. Several remedies for this problem, short of switching to a stainless steel or a high-nickel alloy cladding, are available.

Stresses in the operating hydride fuel pellet arise from two sources: thermal stress (with a variable coefficient of thermal expansion) and stresses developed by the combination of hydrogen redistribution and the variation of fuel density with H/Zr ratio. These components act in opposing directions: thermal stresses are compressive near the center and tensile at the periphery; hydrogen stresses are tensile near the centerline and compressive at the surface. The total stress is the sum of these two components. With helium in the fuel-cladding gap, all three stress components are less than the fracture stress (which, however, is poorly known). With the gap filled with a liquid metal, the tensile axial component exceeds the nominal fracture stress over the interval $0.2 < r/R < 0.7$. This confined stress state will probably not cause pellet cracking.

Axial redistribution of hydrogen is significant, and potentially could affect the neutronics of the hydride-fueled reactor. However, the time to achieve the final steady-state distribution may be much longer than in-reactor fuel lifetimes. A full transient analysis is needed to settle this matter.

Finally, the effects of the separate uranium metal phase, which occupies a volume fraction of 0.21 in the fuel, on the mechanical and thermal properties are unknown.

Appendix A. Thermal stresses with variable coefficient of thermal expansion

The generalized Hooke's law in cylindrical coordinates, including thermal expansion, is

$$\varepsilon_r = \frac{1}{E}[\sigma_r - \nu(\sigma_\theta + \sigma_z)] + \alpha\Delta T, \tag{A.1}$$

$$\varepsilon_\theta = \frac{1}{E}[\sigma_\theta - \nu(\sigma_r + \sigma_z)] + \alpha\Delta T, \tag{A.2}$$

$$\varepsilon_z = \frac{1}{E}[\sigma_z - \nu(\sigma_r + \sigma_\theta)] + \alpha\Delta T, \tag{A.3}$$

where E is Young's modulus, ν is Poisson's ratio and α is the linear coefficient of thermal expansion, which is assumed to be a linear function of temperature but independent of the H/Zr ratio. ΔT is the numerator of Eq. (1). Plane strain is assumed, so that ε_z is a constant. The relation between the strain components is

$$\frac{\mathrm{d}\varepsilon_\theta}{\mathrm{d}r} + \frac{\varepsilon_\theta - \varepsilon_r}{r} = 0. \tag{A.4}$$

Substituting Eqs. (A.1) and (A.2) into Eq. (A.4) yields:

$$\frac{\mathrm{d}}{\mathrm{d}r}[\sigma_\theta - \nu(\sigma_r + \sigma_z)] + E\frac{\mathrm{d}}{\mathrm{d}r}(\alpha\Delta T) + \frac{1+\nu}{r}(\sigma_\theta - \sigma_r) = 0. \tag{A.5}$$

Taking the derivative of Eq. (A.3) and substituting $\mathrm{d}\sigma_z/\mathrm{d}r$ into Eq. (A.5) yields, after the usual manipulation,

$$\frac{1}{r^3}\frac{\mathrm{d}}{\mathrm{d}r}\left(r^3\frac{\mathrm{d}\sigma_r}{\mathrm{d}r}\right) = -\frac{E}{1-\nu}\frac{1}{r}\frac{\mathrm{d}}{\mathrm{d}r}(\alpha\Delta T), \tag{A.6}$$

which differs from the standard starting equation in that the coefficient of thermal expansion cannot be removed from the derivative.

The dimensionless temperature difference is defined by

$$\Delta T/\Delta T_0 = 1 - \eta^2, \tag{A.7}$$

where $\Delta T_0 = T_0 - T_S$ and $\eta = r/R$.

Inserting Eq. (8) for α into Eq. (A.6) yields:

$$\frac{\mathrm{d}}{\mathrm{d}\eta}\left(\eta^3\frac{\mathrm{d}S_r^{\mathrm{th}}}{\mathrm{d}\eta}\right) = -\eta^2\frac{\mathrm{d}}{\mathrm{d}\eta}\left\{[A + B(1-\eta^2)](1-\eta^2)\right\}, \tag{A.8}$$

where S_r^{th} is the dimensionless form of the radial thermal stress:

$$S_r^{\mathrm{th}} = \frac{\sigma_r}{\left(\frac{E\alpha_0\Delta T_0}{1-\nu}\right)} \tag{A.9}$$

and

$$A = 1 + aT_S; \quad B = a\Delta T_0. \tag{A.10}$$

The boundary conditions are

$$\mathrm{d}S_r^{\mathrm{th}}/\mathrm{d}\eta = 0 \quad \text{at } \eta = 0 \quad \text{and} \quad S_r^{\mathrm{th}} = 0 \quad \text{at } \eta = 1. \tag{A.11}$$

Integrating Eq (A.8) twice results in:

$$S_r^{\mathrm{th}} = -\frac{1}{4}(A + 2B)(1-\eta^2) + \frac{1}{6}B(1-\eta^4). \tag{A.12}$$

For a constant thermal expansion coefficient, $a = 0$, $A = 1$ and $B = 0$ and Eq. (A.12) reduces to $S_r^{\mathrm{th}} = -1/4(1-\eta^2)$, which is the standard solution for the thermal stress caused by a parabolic temperature distribution in a solid cylindrical pellet. The equilibrium condition,

$$\frac{\partial}{\partial r}(r\sigma_r) - \sigma_\theta = 0 \tag{A.13}$$

is used to determine the hoop stress:

$$S_\theta^{\text{th}} = -\frac{1}{4}(A + 2B)(1 - 3\eta^2) + \frac{1}{6}B(1 - 5\eta^4). \tag{A.14}$$

The axial stress is calculated as follows [22]: First the axial stress distribution with the pellet completely restrained axially ($\varepsilon_z = 0$) is determined. Next, the radial average of this stress is calculated. The restraint is then removed, so the desired axial stress is $\sigma_z = \sigma_z^R - \overline{\sigma}_z^R$, where the superscript R indicates the restrained condition. The result is

$$S_z^{\text{th}} = -\frac{1}{2}(1 - 2\eta^2)A - \frac{2}{3}\left(1 - 3\eta^2 + \frac{3}{2}\eta^4\right)B. \tag{A.15}$$

Appendix B. Burnup units for U–Zr hydride fuels

The burnup expressed as a fraction of initial metal atoms (U + Zr) consumed, or FIMA, is defined by

$$\text{FIMA} = \Delta N_{25}/(N_{\text{U}} + N_{\text{Zr}}), \tag{B.1}$$

where ΔN_{25} represents the moles of ^{235}U consumed by fission, N_{U} is the initial total moles of uranium, and N_{Zr} is the moles of zirconium. Dividing by N_{U}, the burnup can be expressed as the 'fraction of initial uranium atoms' consumed:

$$\Delta N_{25}/N_{\text{U}} = (1 + N_{\text{Zr}}/N_{\text{U}}) \times \text{FIMA}. \tag{B.2}$$

In conventional burnup units:

$$\begin{aligned}\text{BU (MW d/kg U)} &= 950(\Delta N_{25}/N_{\text{U}}) \\ &= 950(1 + N_{\text{Zr}}/N_{\text{U}}) \times \text{FIMA}.\end{aligned} \tag{B.3}$$

Another measure of burnup of hydride fuels is 'fraction of initial U-235 consumed'. This is given by

$$\frac{\Delta N_{25}}{N_{25}^0} = \frac{N_{\text{U}}}{N_{25}^0} \times \frac{\Delta N_{25}}{N_{\text{U}}} = \frac{\text{FIMA}}{q} \times \left(1 + \frac{N_{\text{Zr}}}{N_{\text{U}}}\right), \tag{B.4}$$

where q is the uranium enrichment.

All conversions require knowledge of the zirconium-to-uranium atom ratio. The literature usually expresses the total uranium content of hydride fuel in terms of weight percent (based on metals only). Thus, fuel with 10 wt% uranium is equivalent to $N_{\text{Zr}}/N_{\text{U}} = 24$, and 45 wt% converts to $N_{\text{Zr}}/N_{\text{U}} = 3.2$.

References

[1] E. Greenspan, H. Garkisch, J. Malen, M. Moalem, D. Olander, B. Petrovic, Z. Shayer, N. Todreas, Trans. Am. Nucl. Soc. 89 (2003) 381.
[2] M.T. Simnad, Nucl. Eng. Des. 64 (1981) 403.
[3] R. Chesworth, G. West, Final Results of Qualification Testing of TRIGA Fuel in the Oak Ridge Research Reactor (ORR), Paper Presented at the International Meeting on Reduced Enrichment for Research and Test Reactors, Petten, Netherlands, 1985.
[4] C. Toma et al., Characterization of TRIGA LEU Fuel Behavior in 14 MW Core, un-numbered report, Institute for Nuclear Research, Pitesti, Romania.
[5] D. Wongsawaeng, D. Olander, Liquid-Metal Bonding of the Fuel-Cladding Gap in Light-Water Reactors, International Meeting on Light-Water Reactor Fuel Performance, Orlando, FL, 2004.
[6] A.F. Lillie et al., USAEC Report AI-AEC-13084, Atomics International, 1973.
[7] G. West, M. Simnad, G. Copeland, Final Results from TRIGA LEU Fuel Postirradiation Examination and Evaluation Following Long-Term Irradiation Testing in the ORR, General Atomics report GA-A18641, 1986.
[8] Yeon Soo Kim, G. Hofmann, Nucl. Technol., submitted for publication.
[9] GA Technologies, Inc. Uranium–Zirconium Hydride TRIGA LEU Fuel, Appendix I-7, Research Reactor Core Conversion Guidebook, IAEA-TEDOC-643 (date unknown).
[10] V.I. Shcherbak et al., Atomnaya Énergiya 31 (1991) 178.
[11] S. Yamanaka et al., J. Nucl. Mater. 294 (2001) 94.
[12] U. Merten et al., J. Nucl. Mater. 10 (1963) 201.
[13] J. Huang et al., J. Nucl. Sci. Technol. 37 (2000) 887.
[14] A. Sommer, W. Dennison, NAA Report NAA-SR-5066, 1960.
[15] Wei-E. Wang, D.R. Olander, J. Am. Ceram. Soc. 78 (1995) 3323.
[16] L. Libowitz, J. Nucl. Mater. 5 (1962) 228.
[17] G. Eggers, Method of Making ZrH Fuel Element, US Patent 4,071,587, column 2, 1978.
[18] U. Merten et al., in: The Proceedings of the Second Conference On Peaceful Uses of Atomic Energy, P/789, Geneva, 1958.
[19] J.D. Gylfe et al., Evaluation of Zirconium Hydride as Moderator in Integral Boiling-Water Superheat Reactors, NAA-SR-5943, 1960, p. 11.
[20] C.F. Bonilla, Nuclear Engineering, McGraw-Hill, 1957, 566 p.
[21] R. Montgomery, R. Yang, Topical Report on Reactivity-Initiated Accidents: Bases for RIA Fuel and Core Coolability Criteria, Figs. 3–12, EPRI 1002865, 2002.
[22] H. Rust, Nucl. Power Plant Eng. (1979) 395.